

## Electronic transport and optical properties of plastically deformed CdS

P. Merchant and C. Elbaum

*Department of Physics and Metals Research Laboratory, Brown University, Providence, Rhode Island 02912*

(Received 10 October 1978)

The temperature dependence of the dc electrical conductivity (300–30°K) and the optical transmission (300–109°K) of plastically deformed CdS crystals have been measured for samples deformed up to 25%. The results yield further evidence for the existence of dislocation energy bands located at energies within 0.3 eV of the valence-band top. A simple band model is presented to describe the observed properties of this system.

### I. INTRODUCTION

In a region surrounding a dislocation, the periodicity of a crystal lattice is disturbed. Since the electronic band structure of a crystal depends on the translational invariance of the lattice, a disturbance of this symmetry by the introduction of a large number of dislocations into the crystal, for example, by plastic deformation, may have a significant effect on its electronic transport and optical properties. Such changes can be attributed to special features of the electronic states in regions around dislocations.<sup>1-8</sup>

Experiments on deformed CdS by Elbaum<sup>9</sup> showed the existence of a strongly anisotropic conductivity, the highly conducting direction being parallel to the direction of screw dislocations produced by the deformation. Although screw dislocations do not have unpaired bonds, calculations by Emtage<sup>10</sup> have shown that electrons and holes may be bound to dislocations by a deformation potential<sup>11</sup> resulting from the elastic stress field of a dislocation. In addition to the anisotropic conductivity found by Elbaum<sup>9</sup> he noted that the temperature dependence of the conductivity along the highly conducting direction was suggestive of a Peierls-type transition<sup>12</sup> from a metallic to a semiconducting state as the temperature was decreased.

In the present work the optical and electronic transport properties of two different undeformed and several deformed CdS crystals were measured. A band model formulated earlier accounts for the observed changes in these properties as a result of deformation.

### II. EXPERIMENTAL METHODS

The samples used in these studies consisted of single crystals of CdS grown by the vapor deposition process by the Eagle Picher Co. Although not intentionally doped, all of the samples contained

significant amounts of defects and/or impurities as seen from their dc conductivity and optical transmission (below). Initial orientation was obtained from x-ray Laue backscattering photographs. The specimens were then cut from large single crystals ( $\sim 3 \text{ cm}^3$ ) into rectangular parallelepipeds, measuring approximately  $3 \times 4 \times 5$  mm, along the  $[4\bar{5}10]$ ,  $[0001]$ , and  $[2\bar{1}\bar{3}0]$  directions, respectively.

The plastic deformation was accomplished at a temperature sufficient to facilitate slip; a uniaxial stress was applied along the  $[4\bar{5}10]$  direction, as described earlier.<sup>9</sup> The strain was measured by the percent decrease in sample thickness in the direction of the applied stress (Table I).

After deformation the samples were observed with an optical microscope. x-ray Laue backscattering photographs were taken for representative samples to determine the nature of the slip processes which had occurred. To accomplish this, consistency was sought between the possible slip process and the rotation of the Laue spots, which resulted from deformation.

Measurements of the electrical conductivity  $\sigma(T)$  (in the dark) were made by the two-point probe method,<sup>9,13</sup> using a Keithley electrometer (Model 610A). Earlier experiments had demonstrated that the results of this method agreed with those found by the four-point probe method whenever the contacts showed ohmic behavior.<sup>9</sup> Measurements of the Hall constant and determination of majority carrier type were made for one of the undeformed samples (CdS 0%, batch II), along the  $[0001]$  and  $[2\bar{1}\bar{3}0]$  directions at 297°K and 77°K.

The optical transmitted and reflected intensities of the samples were obtained using two spectrometer systems. A rapid-scanning Fourier-transform spectrometer (FTS-14, Digilab) was used in the far-infrared (far-ir) region of the spectrum, 0.0062–0.37 eV; and a dual beam spectrometer (Cary 17) in the near infrared

TABLE I. Deformation parameters for samples of CdS.

Samples	% def.	Area (mm <sup>2</sup> )	Full stress (kg/mm <sup>2</sup> )	$T_D$ (°C)	$t_D$ (min)
Batch I					
CdS 1	25	16.96	3.18	607	20
CdS 2	25	16.87	3.11	605	20
Batch II					
CdS B	11	17.14	2.10	598	20
CdS C	21	15.05	3.19	598	20
CdS D	22	15.15	3.19	605	60

(near ir) through the ultraviolet (uv) regions of the spectrum, 0.496–3.82 eV. In order to obtain spectra free of the effects of diffuse surface scattering of the beam, the samples were polished with a series of Buehler Al<sub>2</sub>O<sub>3</sub> powders suspended in distilled water (12.0, 5.0, 1.0, 0.3, and 0.05- $\mu$ m grit size) prior to measurement of the transmission or reflectivity spectra. For temperature-dependent measurements, spectra were taken during the cooling cycle, the rate being about 5°K/min for temperatures above 150°K, and as slow as 1°K/10 min below about 120°K. When the cooling was rapid, the temperatures were recorded at evenly spaced wavelength intervals during a scan.

### III. EXPERIMENTAL RESULTS

#### A. CdS-Batch I

The undeformed samples of CdS batch I were characterized by a uniform yellow color and an isotropic dc electrical conductivity (in the dark) having a magnitude on the order of  $10^{-6}$  ( $\Omega$  cm)<sup>-1</sup> at room temperature.

Deformation resulted in an elongation in the [21 $\bar{3}$ 0] direction, contraction in the [4 $\bar{5}$ 10] direction and less than a 0.5% change in length along the [0001] direction. From the rotation of Laue spots after deformation, it was determined that the deformation of the CdS samples was consistent with glide on the ( $\bar{1}$ 100) planes in the [11 $\bar{2}$ 0] direction. This deformation produces edge dislocations along the [0001] direction and screw dislocations along the [11 $\bar{2}$ 0] direction.<sup>14</sup> A non-uniform coloration seen in the deformed samples had the appearance of reddish-brown spots near the corners of the (0001) face, with a nearly continuous, lighter smearing of this color connecting diagonally opposed spots. When viewed along the [4 $\bar{5}$ 10] direction with a polarizing filter, this coloration is only visible for light polarized parallel to the [21 $\bar{3}$ 0] direction.

After deformation extensive changes were found in the dc conductivity of these samples.<sup>9</sup> Along the [21 $\bar{3}$ 0] direction  $\sigma$  had increased to 3 ( $\Omega$  cm)<sup>-1</sup> at room temperature and its temperature dependence showed a transition from a metallic to a semiconducting state at 125°K. The conductivity along the [4 $\bar{5}$ 10] and [0001] directions remained unchanged at room temperature, but decreased monotonically as the temperature was lowered so that at 125°K the anisotropy in the conductivity was in excess of 10<sup>3</sup>. These features were found to remain unchanged two years after the deformation was carried out.

Figure 1 shows the results of far-ir reflectivity measurements at room temperature for CdS 2 (25%), in the range 85–10<sup>3</sup> cm<sup>-1</sup>, for light polarized parallel to the [21 $\bar{3}$ 0] [Fig. 1(a)] and [0001] [Fig. 1(b)] crystallographic directions. Similar results were found for the undeformed sample. The most noticeable feature in these plots is the reststrahlen band in the 200–300 cm<sup>-1</sup> region which is due to lattice absorption by transverse and longitudinal optical phonons.<sup>15</sup> Results similar to those presented in Fig. 1 were also seen for the reflectivities of both samples of this batch at 80°K, the only change in the spectra being a sharpening of the reststrahlen band edge. At higher photon energies transmission measurements of the samples of batch I show a continuous increase from 5% at 600 cm<sup>-1</sup> to 80% at 14260 cm<sup>-1</sup>.

The room-temperature polarized transmission spectrum of CdS 1 (25%) in the visible region of the spectrum is presented in Fig. 2. The transmitted intensity, for light polarized parallel  $T_{\parallel}$  and perpendicular  $T_{\perp}$  to the (hexagonal)  $c$  axis show the birefringence due to the crystal field and spin-orbit splitting of the  $\Gamma_7$  and  $\Gamma_9$  valence bands. In the 2.03–2.40-eV region  $T_{\perp}$  has a broad absorption knee. Measurements of the transmission at other polarization orientations show that the depth of this knee is maximum for

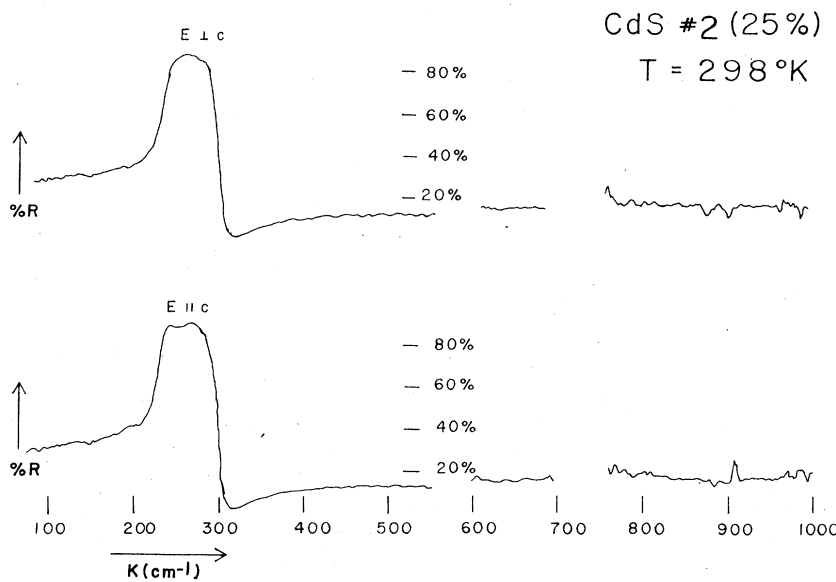


FIG. 1. Room-temperature far-ir polarized reflectivities of CdS 2, batch I. (a)  $\vec{E} \perp \vec{c}$ , (b)  $\vec{E} \parallel \vec{c}$ . The spectra are not plotted in regions of low signal-to-noise ratio.

$T_{\perp}$ . It does not appear in the undeformed samples of CdS or in other studies of the transmission of CdS in this spectral region<sup>16</sup>; however, it has been seen to have the same shape and location in similarly deformed samples of CdS.<sup>17</sup>

B. CdS-Batch II

A second batch of CdS crystals was prepared starting with a different single crystal from that used for CdS batch I. The dc electrical conductivity of one of the undeformed samples of this batch, CdS A (0%), is shown in Fig. 3. The

values of the conductivities of this sample along the  $[21\bar{3}0]$  and  $[0001]$  directions are  $0.15$  and  $0.36 (\Omega \text{ cm})^{-1}$ , respectively, at room temperature. This anisotropy is within the uncertainty of the wetted areas of the contacts. The temperature dependence of  $\sigma$  may be divided into two parts. Above about  $140^{\circ}\text{K}$ ,  $\sigma$  decreases with temperature as  $T^{-n}$ , with  $n$  being  $1.0$  and  $1.4$  for the  $[21\bar{3}0]$  and  $[0001]$  directions, respectively. For both directions,  $\sigma$  goes through a maximum at  $115 \pm 5^{\circ}\text{K}$ , and for temperatures below  $115^{\circ}\text{K}$ ,  $\sigma$  decreases exponentially with decreasing temperature as  $\sigma_0 e^{-\Delta/k_B T}$ , with the activation energies

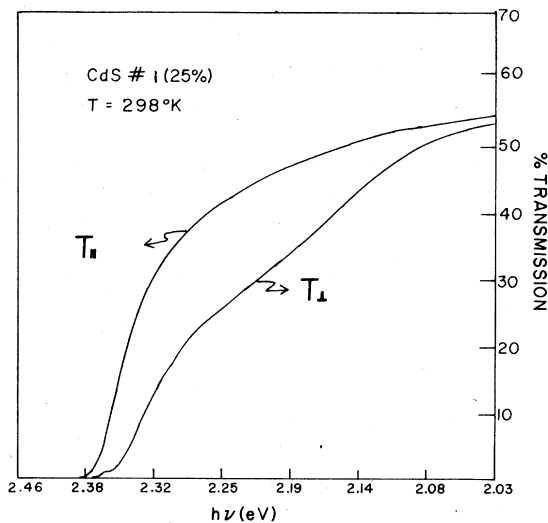


FIG. 2. Room-temperature polarized transmission of CdS 1, batch I for  $\vec{E} \parallel \vec{c}$  and  $\vec{E} \perp \vec{c}$ .

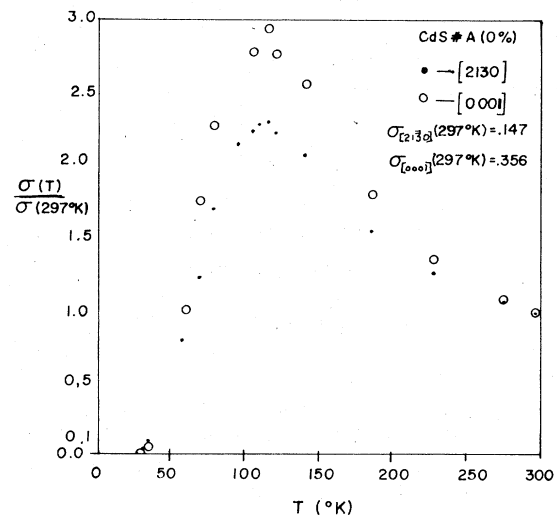


FIG. 3. Normalized dc electrical conductivity of CdS A, batch II. Solid circles,  $[21\bar{3}0]$  direction; open circles,  $[0001]$  direction.

TABLE II. Summary of the conductivity measurements of CdS batch II. Values of  $\sigma$  are in  $(\Omega \text{ cm})^{-1}$ ;  $T = 296^\circ\text{K}$ .

Sample No. \\ (% deformation)	$\sigma_{[21\bar{3}0]}$	$\sigma_{[0001]}$	$\sigma_{[4\bar{5}10]}$	$T_p$ ( $^\circ\text{K}$ )	$\Delta$ (eV) \\ [21 $\bar{3}0$ ]	$\Delta$ (eV) \\ [0001]
CdS A (0%)	0.147	0.356	...	115 $\pm$ 5	0.017	0.020
CdS B (11%)	<10 <sup>-7</sup> <sup>a</sup>	<10 <sup>-7</sup> <sup>a</sup>	<10 <sup>-7</sup> <sup>a</sup>	...	...	...
CdS C (21%)	0.0136	0.0070	<10 <sup>-6</sup> <sup>a</sup>	130 $\pm$ 10	0.017	0.015
CdS D (22%)	0.048	0.0071	2.3 $\times$ 10 <sup>-6</sup>	130 $\pm$ 10	0.015	0.012

<sup>a</sup> Nonohmic contacts prevented more than an order of magnitude estimate of  $\sigma$ .

being  $\Delta_{[0001]} = 0.020$  eV and  $\Delta_{[21\bar{3}0]} \approx 0.017$  eV. The Hall effect in this sample was also measured at room temperature and at 77°K, along the [0001] and [21 $\bar{3}0$ ] directions, since the contacts used for measuring  $\sigma(T)$  were ohmic. At both temperatures and along both directions it was found that the majority carriers were electrons. The carrier concentration,  $n$  ( $\text{cm}^{-3}$ ), and electron Hall mobilities,  $\mu_n$  ( $\text{cm}^2/\text{V sec}$ ), were found under the assumption that only electrons contribute to the observed conductivity for this sample,  $n \gg p$ . The results are:  $n_{297\text{K}} \approx 2 \times 10^{16}$ ;  $n_{77\text{K}} \approx 7 \times 10^{15}$ ;  $\mu_{297\text{K}} \approx 60$ ;  $\mu_{77\text{K}} \approx 500$ .

In the far-ir region of the spectrum, polarized reflectivity for 50–200  $\text{cm}^{-1}$  and unpolarized transmission and reflectivity in the 400–2800  $\text{cm}^{-1}$  region were measured at room temperature for CdS A (0%). The reflectivity plots for 50–10<sup>3</sup>  $\text{cm}^{-1}$  show no differences from the results presented in Fig. 1. From 1000–2800  $\text{cm}^{-1}$  the unpolarized reflectivity is nearly constant, 20  $\pm$  4%, with no apparent structure. The corresponding transmitted intensity in this region increases from less than 5% at 600  $\text{cm}^{-1}$  to 40% at 2000  $\text{cm}^{-1}$ . A continuation of the transmission through the near ir shows a continued smooth increase to about 80% at 7000 Å (1.77 eV). Polarized transmission and reflectivity of CdS A (0%), in the visible region of the spectrum (7000–4000 Å) have been reported earlier.<sup>13</sup> Estimates of the energy gap 2.38 eV and the crystal field and spin-orbit splitting of the  $\Gamma_9$  and upper  $\Gamma_7$  valence bands, 0.016  $\pm$  0.002 eV, are obtained from an extrapolation of the transmission curves (for transmissions less than 10%), to the  $h\nu$  axis. Previously reported values for these parameters at 297°K are 2.43 and 0.015 eV, respectively.<sup>16</sup>

Deformation of CdS batch II was similar to that of CdS batch I. Investigations of the 11% and 21% and 22% deformed samples of CdS batch II revealed no significant changes in the far- and near-ir properties from that seen in CdS A (0%). However, significant changes were observed in

the electronic transport and visible range optical properties of the deformed samples.

The characteristics of the dc electrical conductivity of all of the CdS samples of this batch are summarized in Table II. Because of non-ohmic contacts in all directions in the 11% deformed sample, and along the [4 $\bar{5}10$ ] direction in the 21% and 22% deformed samples, the conductivity could only be estimated. The maximum value for  $\sigma$  was chosen from the smallest resistance measured, this occurring for the largest applied current, i.e., 10<sup>-7</sup> A. The plots of  $\sigma(T)$  for the 22% deformed sample are presented in Fig. 4. It can be seen from these plots and from Table II that after deformation there are several significant changes in the conductivity from that observed in the undeformed sample; (i) the temperature of the conductivity peak,  $T_p$ , has shifted from 115 to 130°K in the 21% and 22% deformed samples; (ii) for both the [21 $\bar{3}0$ ] and the [0001] directions the activation energy for the conductivity decreases monotonically with the amount of plastic strain; (iii) the conductivity along the [4 $\bar{5}10$ ] direction has decreased to 2.3  $\times$  10<sup>-6</sup> ( $\Omega \text{ cm}$ )<sup>-1</sup> at 297°K; (iv) at 130°K the anisotropy is approximately 10<sup>4</sup>.

The results of room-temperature polarized

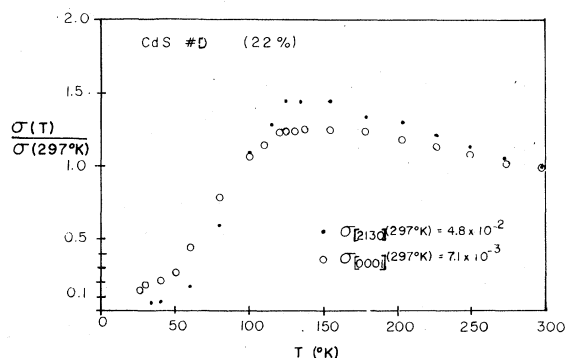


FIG. 4. Normalized dc electrical conductivity of CdS D, batch II. Room-temperature values of  $\sigma$  are in  $(\Omega \text{ cm})^{-1}$ .

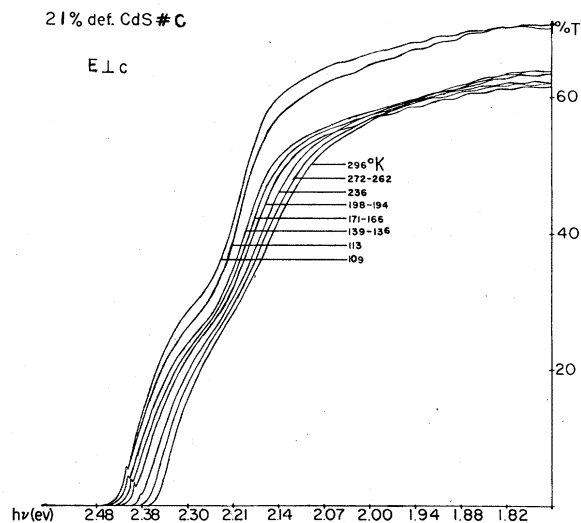


FIG. 5. Temperature-dependent polarized transmission of CdS C, batch II for  $\vec{E} \perp \vec{c}$ .

transmission and reflectivity measurements in the visible region of the spectrum for the undeformed, 11% and 21% deformed samples of this batch of samples have been presented earlier.<sup>13</sup> We wish to add that there is no observed narrowing of the energy gap by 0.1 eV in the deformed samples as reported by Klassen and Osip'yan.<sup>17</sup> Finally, for CdS batch II, the temperature dependence of the transmission of the 21% deformed sample for light polarized parallel to the [2130] direction is shown in Fig. 5. Note that the knee in the transmission occurring in the 2.1–2.3 eV region at 296°K becomes larger as the temperature is decreased; and that below the transition temperature for the conductivity,  $130 \pm 10^\circ\text{K}$ , the transmission on the low-energy side of this knee increases by about 10%.

#### IV. DISCUSSION OF RESULTS

##### A. CdS-Batch I

From the conductivity measurements on the undeformed samples of this batch it is known that there exist in the fundamental gap defect states which determine the electrical properties of these samples. The isotropy of the conductivity indicates the absence of a significant excess density of dislocation lines along any particular direction in the undeformed samples.

In an earlier Letter,<sup>9</sup> it was proposed that during deformation these samples acquired the characteristics of a pseudo-one-dimensional system. From an assumed screw dislocation density of  $10^{10}$  lines/cm<sup>2</sup> and dislocation radius of  $5 \times 10^{-8}$  cm, the conductivity along the screw

dislocations was estimated to be on the order of  $10^5$  ( $\Omega \text{ cm}$ )<sup>-1</sup> at 125°K. The magnitude and temperature dependence of this conductivity is therefore similar to that seen in the highly conducting organic complexes  $\text{K}_2\text{Pt}(\text{CN})_4\text{Br}_{0.3} \cdot (\text{H}_2\text{O})_n$  (KCP),<sup>18</sup> and tetrathiafulvalenium-tetracyanoquinodimethanide (TTF-TCNQ).<sup>19</sup> Optical experiments on KCP,<sup>18,20,21</sup> and TTF-TCNQ,<sup>22,23</sup> have shown that above the transition temperature the metallic conduction is also evident as a highly anisotropic reflectivity for photon energies below the plasma edge.<sup>18,20-23</sup> Therefore, similar effects were looked for in the deformed CdS samples of this batch. In addition, if a Peierls gap opens in the screw dislocation band at low temperatures, it may be observable by interband transitions across this gap, which for our samples was estimated to be  $\sim 0.015$  eV ( $123 \text{ cm}^{-1}$ ).<sup>24</sup>

A comparison of Figs. 1(a) and 1(b) shows that for CdS 2 (25%) the anisotropy in the reflectivity is  $1.0 \pm 0.2$  throughout the  $85\text{--}10^3 \text{ cm}^{-1}$  region, much less than that seen for the KCP and TTF-TCNQ complexes. This fact suggests that either the plasma edge for carriers in the dislocation band is less than 0.010 eV ( $85 \text{ cm}^{-1}$ ), implying a corresponding carrier density  $n \leq 8 \times 10^{16} \text{ cm}^{-3}$  in this band, or that, due to the small volume fraction of dislocations,  $V_D$ , in this crystal ( $V_D < 10^{-4}$  of the total crystal volume for the dislocation density and radius assumed above), the lattice absorption of the bulk material dominates the far-ir properties of these samples. Measurements of the optical properties of these samples in the 4000–7000 Å region (below) seem to rule out the former interpretation. From reflectivities of these samples taken at 80°K for the same polarization and spectral region, again there was no evidence of interband absorption across a Peierls gap in the  $123\text{-cm}^{-1}$  region.

The most direct evidence for the existence of a dislocation band in deformed CdS is the knee in the  $T_{\perp}$  curve of Fig. 2. Since it does not appear in undeformed CdS, it is obviously connected with the deformation process and perhaps with transitions of holes or electrons from the dislocation band to the valence or conduction band. The calculated absorption coefficient for this knee is on the order of  $10 \text{ cm}^{-1}$  compared to values on the order of  $10^4$  to  $10^5 \text{ cm}^{-1}$  for direct valence to conduction band transitions. If the densities of initial and final states scale accordingly for these two transitions, then a density of states of  $10^{19}\text{--}10^{20} \text{ cm}^{-3}$  contributes to the knee absorption. Note that this density is much greater than that expected if the plasma edge is below 0.010 eV ( $85 \text{ cm}^{-1}$ ) in the far ir.

## B. CdS-Batch II

As for the undeformed samples of batch I, the observed conductivity for the undeformed sample of batch II is suggestive of a thermal activation of carriers from impurity or defect levels into a conduction band. The portion of the curves (Fig. 3) for  $T > 115^\circ\text{K}$  is suggestive of phonon and impurity scattering effects for normal band conduction, i.e., the  $T^{-1}$  dependence of  $\sigma$ . From additional electronic transport properties of this sample, listed previously, two features are apparent. (a) The carrier concentration in this sample changes only by a factor of about 4 from 77 to  $298^\circ\text{K}$ , which is indicative of an excitation of carriers from a series of levels close to the conduction band. (b) The low Hall mobility of these carriers<sup>25</sup> is also indicative of extensive impurity scattering.

An idea of the distribution of the impurity and/or defect states in the gap of the undeformed samples can be found from the far-ir-near-ir transmission of CdS A (0%). From the smooth increase in transmission from 5% at  $600\text{ cm}^{-1}$  to 80% at  $14260\text{ cm}^{-1}$  it appears that the optical absorption decreases as the photon energies increase below the gap energy, indicating that the population of impurity and/or defect states is larger near the band edges than it is near the middle of the gap. The transmission measurements of this sample in the visible region,<sup>13</sup> show that in the 2.0–2.38 eV range the transmission decreases rapidly as the gap energy is approached, as expected for a distribution of unoccupied donor and occupied acceptor states located near the band extrema. The facts that the electrical conductivity has an activation energy of 0.017–0.020 eV and that the large increase in optical absorption occurs in the range 2.0–2.38 eV imply that the acceptor levels occupy a region within  $\sim 0.40$  eV of the valence band.

The changes in the electrical conductivity of the deformed samples of batch II, shown in Table II, indicate a significant change in the electronic transport properties resulting from plastic deformation. Of the features listed in Sec. III above (i) and (ii) suggest that there has been a change in the level spacing or carrier population in the impurity or defect levels below the conduction band; however, the small conductivity of the 11% deformed sample and the measured anisotropy, cannot be explained by such a small shift in shallow state energies. A more likely explanation is that during deformation, dislocations are produced which have acceptor levels near the valence band top. As the dislocation density increases, so does the com-

ensation of the donor levels by these acceptors. The emptying of the donor levels then lowers the conductivity as seen in the 11% deformed sample. Further deformation results in a further increase in the dislocation acceptor state density and a further filling of these states, leading to a band formation and conduction along the screw and edge dislocations for sufficient electron densities in the dislocation bands.

Further support for this model comes from the polarized transmission and reflectivity spectra of the 11% and 21% deformed samples in the visible region of the spectrum. As mentioned earlier,<sup>13</sup> the major changes after deformation are the broadening of the absorption edge and the appearance of a knee in the  $T_{\perp}$  curves in the 2.1–2.3 eV region in the deformed samples, similar to those seen in Fig. 2 for the 25% deformed sample of batch I. Of particular interest is the scaling of the absorption of the 2.1–2.3 eV region with the amount of plastic strain and hence a monotonic dependence of this absorption on the dislocation density.<sup>13</sup> From the temperature dependence of  $T_{\perp}$  for CdS C (20%), shown in Fig. 5, the following interpretation is suggested. The width of the knee, and its growth as the temperature decreases are similar to those seen for phonon broadening of impurity levels.<sup>26</sup> The decreased absorption below the low-energy side of the knee upon lowering the temperature, may be interpreted as the freezing out of carriers from acceptor levels which take part in transitions to the conduction band at high temperatures.

A band structure model which consistently describes all of the above effects is presented in Fig. 6.

In this model we assume unoccupied acceptor

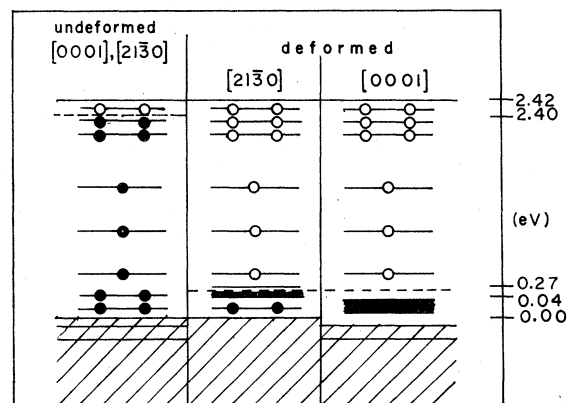


FIG. 6. Proposed band model for undeformed and deformed CdS at the  $\Gamma$  point ( $k=0$ ). Open circles represent unoccupied donor and acceptor levels within the gap. Closed circles represent occupied states.

levels located at energies above the dislocation band top unlike in an earlier model.<sup>13</sup> Before deformation, these acceptor levels are occupied and therefore contribute to optical absorption in the 2.0–2.4 eV region. After deformation they serve as a mechanism by which the dislocation bands can be partially emptied by thermal excitation, allowing conductivity to occur in the (unfilled) dislocation bands at high temperatures. Since these levels are separated from the valence band by  $\sim 0.3$  eV, their effects on the conductivity along the  $[4510]$  direction is minimal.

In conclusion, the changes in the electronic transport and optical properties of CdS resulting

from plastic deformation have been described in terms of a model in which dislocation energy bands are created during the deformation process. A screw dislocation band has been found to lie between approximately 0.04 and 0.27 eV above the valence band top and an edge dislocation band has been found to lie at slightly lower energies.

#### ACKNOWLEDGMENTS

The authors wish to thank T. Kirst for assistance in taking some of the optical measurements. Research supported in part by the NSF through the Materials Research Laboratory of Brown University.

- 
- <sup>1</sup>W. Shockley, *Phys. Rev.* **91**, 228 (1953).  
<sup>2</sup>W. T. Read, Jr., *Philos. Mag.* **45**, 775 (1954).  
<sup>3</sup>W. T. Read, Jr., *Philos. Mag.* **45**, 1119 (1954).  
<sup>4</sup>W. T. Read, Jr., *Philos. Mag.* **46**, 111 (1955).  
<sup>5</sup>R. A. Logan, G. L. Pearson, and S. A. Kleinman, *J. Appl. Phys.* **30**, 885 (1959).  
<sup>6</sup>V. L. Bonch-Bruyevich and V. B. Glasko, *Sov. Phys. Solid State* **3**, 26 (1961) [*Fiz. Tverd. Tela* **3**, 36 (1960)].  
<sup>7</sup>Y. V. Galyaev, *Sov. Phys. Solid State* **3**, 796 (1961) [*Fiz. Tverd. Tela* **3**, 1094 (1960)].  
<sup>8</sup>R. R. Holmes and C. Elbaum, *Phys. Rev.* **173**, 803 (1968).  
<sup>9</sup>C. Elbaum, *Phys. Rev. Lett.* **32**, 376 (1974).  
<sup>10</sup>P. R. Emtage, *Phys. Rev.* **163**, 865 (1967).  
<sup>11</sup>W. Shockley and J. Bardeen, *Phys. Rev.* **77**, 407 (1950); J. Bardeen and W. Shockley, *Phys. Rev.* **80**, 72 (1950).  
<sup>12</sup>R. E. Peierls, *Quantum Theory of Solids* (Oxford University, Oxford, England, 1953), p. 108.  
<sup>13</sup>P. Merchant and C. Elbaum, *Solid State Commun.* **20**, 775 (1976).  
<sup>14</sup>Y. A. Osipyan and I. S. Smirnova, *Phys. Status. Solidi* **30**, 19 (1968).  
<sup>15</sup>B. Ray, *II-VI Compounds* (Pergamon, New York, 1971), p. 64.  
<sup>16</sup>Reference 15, Chap. 3.  
<sup>17</sup>N. V. Klassen and Y. A. Osip'yan, *Sov. Phys. Solid State* **14**, 3094 (1973) [*Fiz. Tverd. Tela* **14**, 3694 (1972)].  
<sup>18</sup>D. Kuse and H. R. Zeller, *Phys. Rev. Lett.* **27**, 1060 (1971).  
<sup>19</sup>L. B. Coleman, M. J. Cohen, D. J. Sandman, F. G. Yamagishi, A. F. Garito, and A. J. Heeger, *Solid State Commun.* **12**, 1125 (1973).  
<sup>20</sup>P. Bruesh and F. Lehman, *Solid State Commun.* **10**, 579 (1972).  
<sup>21</sup>A. Wagner, H. P. Gersach, R. V. Blatz, and K. Krogmann, *Solid State Commun.* **13**, 659 (1973).  
<sup>22</sup>A. A. Bright, A. F. Garito, and A. J. Heeger, *Solid State Commun.* **13**, 943 (1973).  
<sup>23</sup>P. M. Grant, R. L. Greene, G. C. Wrighton, and G. Castro, *Phys. Rev. Lett.* **31**, 1311 (1973).  
<sup>24</sup>Using the energy gap 0.018 eV as the Peierls gap parameter, its width at 80°K was estimated from a schematic diagram of the temperature dependence of the gap width appearing in M. J. Rice and S. Strassler, *Solid State Commun.* **13**, 125 (1973).  
<sup>25</sup> $\mu_H$  (300°K)  $\sim 300$  cm<sup>2</sup>/√V sec in pure CdS; H. Fugita, K. Kobayashi, T. Kawai, and K. Shiga, *J. Phys. Soc. Jpn.* **20**, 109 (1965).  
<sup>26</sup>M. Lax and E. Burstein, *Phys. Rev.* **100**, 592 (1955).